Norrman, B., Wallen, P., & Ranby, M. (1985) *Eur. J. Biochem. 149*, 193–200.
Pennica, D., Holmes, W. E., Kohr, W. J., Harkins, R. N., Vehar, G. A., Ward, C. A., Bennett, W. F., Yelverton, E., Seeburg, P. H., Heyneker, H. L., Goeddel, D. V., & Collen, D. (1983) *Nature (London) 301*, 214–221.
Radcliffe, R., & Heinze, T. (1978) *Arch. Biochem. Biophys. 189*, 185–194.
Ranby, M., Bergsdorf, N., & Nilsson, T. (1982) *Thromb. Res. 27*, 175–183.
Rijken, D. C., & Collen, D. (1981) *J. Biol. Chem. 256*, 7035–7041.
Rijken, D. C., Hoylaerts, M., & Collen, D. (1982) *J. Biol. Chem. 257*, 2920–2925.
Rijken, D. C., Juhan-Vague, I., DeCock, F., & Collen, D. (1983) *J. Lab. Clin. Med. 101*, 274–284.
Suenson, E., & Peterson, L. C. (1986) *Biochim. Biophys. Acta 870*, 510–519.
Suenson, E., Lutzen, O., & Thorsen, S. (1984) *Eur. J. Biochem. 140*, 513–522.
Tate, K. M., Higgins, D. L., Holmes, W. E., Winkler, M. E., Heyneker, H. L., & Vehar, G. A. (1987) *Biochemistry 26*, 338–343.
Thorsen, S., Glas-Greenwalt, P., & Astrup, T. (1972) *Thrombos. Diath. Haemorrh. 28*, 65–74.
Tran-Thang, C., Kruithof, E. K. O., & Bachmann, F. (1984) *J. Clin. Invest. 74*, 2009–2016.
Tran-Thang, C., Kruithof, E. K. O., & Bachmann, F. (1986) *Eur. J. Biochem. 160*, 599–604.
Vallee, B. L., & Hoch, F. D. (1955) *Proc. Natl. Acad. Sci. U.S.A. 83*, 4670–4674.
van Zonneveld, A. J., Veerman, H., & Pannekoek, H. (1986) *J. Biol. Chem. 261*, 14214–14218.
Verstraete, M., & Collen, D. (1986) *Blood 67*, 1529–1541.
Wallen, P., Ranby, M., Bergsdorf, N., & Kok, P. (1981) *Prog. Fibrinolysis 5*, 16–23.

Neutron Scattering Determination of the Binding of Prothrombin to Lipid Vesicles†

Jim Torbet*
Institut Laue-Langevin, 38042 Grenoble Cedex, France
Jean-Marie Freyssinet
Centre de Transfusion Sanguine, Service d'Hemostase et de Thrombose, Unite 311 INSERM, 67085 Strasbourg Cedex, France
Received March 25, 1987; Revised Manuscript Received July 9, 1987

ABSTRACT: Low-angle neutron scattering is used to study the binding of human prothrombin to small single-bilayer vesicles consisting of phosphatidylcholine and phosphatidylserine (1/1 w/w). The radius of gyration of prothrombin indicates that it is an elongated molecule. The vesicles alone were not observed to coalesce, and their molecular weight, outer radius, and average surface area per lipid were respectively $(1.6 \pm 0.32) \times 10^6$, 114 ± 4 Å, and 110 ± 18 Å^2. These values were independent of the presence of calcium and were not altered significantly by prothrombin, which binds reversibly to the vesicle outer surface with its long axis projecting approximately radially forming a 90-Å thick protein shell. From the titration of the protein–vesicle interaction, the apparent dissociation constant of the binding of prothrombin to these vesicles is estimated to be 0.8 ± 0.4 μM. At saturation, 57 ± 7 prothrombin molecules bind, giving 25 ± 6 lipid residues and an area of 2900 ± 400 Å^2 per prothrombin molecule on the vesicle outer surface. This area is about twice that calculated from a prolate ellipsoid model for prothrombin. However, it is close to the maximum cross-sectional area of fragment 1, the lipid binding region of prothrombin, which is coin-shaped in the high-resolution X-ray structure [Park, C. H., & Tulinsky, A. (1986) *Biochemistry 25*, 3977–3982]. This similarity suggests that prothrombin binding could be sterically limited.

Blood coagulation involves a series of zymogen–enzyme conversions that require protein cofactors, negatively charged phospholipid surfaces, and calcium ions (Jackson & Nemerson, 1980). Thrombin (M_r 37 000), the enzyme that activates fibrinogen prior to its polymerization into fibrin, is produced by proteolytic cleavages of the zymogen prothrombin (M_r 72 000) in the prothrombinase enzymatic complex that includes factor X_a (the enzyme), factor V_a (protein cofactor), phospholipids, and calcium ions (Nesheim & Mann, 1983; Mann, 1984). Prothrombin is a single-chain vitamin K dependent glycoprotein containing approximately 10% carbohydrate and 10 γ-carboxyglutamic acid residues. The latter are involved in the binding of calcium ions, and most if not all are required for complete prothrombin attachment to the membrane surface (Nelsestuen, 1976; Borowski et al., 1985). No specific function for the carbohydrate has been identified. The prothrombin structure can be subdivided into three domains designated fragments 1 and 2 and prethrombin 2 with molecular weights respectively of approximately 21 000, 13 000, and 38 000 (Heldebrant et al., 1973; Owen et al., 1974). The γ-carboxyglutamate residues are on fragment 1 to which are also attached two of the three carbohydrate chains, the third being bound to prethrombin 2. Fragment 1 binds to phospholipid, fragment 2 appears to contain sites involved in interactions with factor V_a and factor X_a, and prethrombin 2 is converted into thrombin by cleavage of a single peptide bond (Mann &

† This work was supported in part by Grant 85-3-21-5-E from CNAMTS and in the initial stages by the Max-Planck-Institut für Festkorperforschung, Hochfeld-Magnetlabor in Grenoble.

0006-2960/87/0426-7791$01.50/0

Elion, 1980; Mann, 1984). At high resolution, fragment 1 has an overall shape of an eccentric oblate ellipsoid of dimensions 11 × 28 × 30 Å (Park & Tulinsky, 1986).

The binding of prothrombin and fragment 1 to phospholipid vesicles (Dombrose et al., 1977; Lim et al., 1977; Nelsestuen & Broderius, 1977; Nelsestuen & Lim, 1977; Resnick & Nelsestuen, 1980; van der Waart et al., 1984; Lintz et al., 1985; Prigent-Dachary et al., 1986) and monolayers (Lecompte et al., 1980; Cuypers et al., 1983; Kop et al., 1984; Mayer et al., 1983) has been investigated with different techniques, conditions, and acidic to neutral phospholipid ratios.

Although in most biomembranes the lipid is less than 20% acidic, we chose vesicles with more than twice this content so that protein binding would not be limited by the availability of charged lipids and in order to avoid the possibility that the properties of the small vesicles used could be modified by, for example, lateral phase separation (Mayer & Nelsestuen, 1981), giving rise to islands of charged lipids interacting with prothrombin in an expanse of neutral lipids (Nelsestuen & Broderius, 1977). Here we use small-angle neutron scattering with contrast variation to study the binding of prothrombin to small single-bilayer lipid vesicles made up of equal proportions of phosphatidylcholine and phosphatidylserine extracted from bovine spinal cord. Titration of the protein–vesicle interaction is reported, and the approximate orientation of the long axis of the elongated prothrombin molecule relative to the membrane surface is ascertained. The results demonstrate that a great deal of information about the attachment of proteins to single-bilayer lipid vesicles can be directly deduced from low-angle scattering. This is especially true when there is little or no penetration of protein into the lipid as with extrinsic membrane proteins.

Materials and Methods

Sample Preparation

The buffer used throughout was 20 mM MOPS [3-(*N*-morpholino)propanesulfonic acid] adjusted to give a reading on the pH meter of 7.5 in H_2O or 7.1 in D_2O in order to account for the deviation in the meter due to deuterium (Kruse et al., 1982). All solutions contained 0.2 M NaCl and 0.01% (w/v) NaN_3 unless otherwise stated. Different H_2O/D_2O ratios were obtained by mixing the solutions. The actual D_2O contents were determined from neutron transmission measurements.

Prothrombin Preparation. Human prothrombin was purified from therapeutic factor II concentrates (Centre Regional de Transfusion Sanguine, Strasbourg, France) by affinity chromatography on dextran sulfate–Sepharose 4B as already described (Freyssinet et al., 1982). At this stage prothrombin was homogeneous when analyzed by sodium dodecyl sulfate–polyacrylamide gel electrophoresis (Laemmli, 1970), but preliminary neutron scattering studies revealed the presence of aggregates even without added calcium, with 1 mM EDTA (ethylenediaminetetraacetic acid) present, at low protein concentration (2 mg/mL) and at high NaCl concentration (0.3 M). In order to eliminate aggregates, these protein preparations were concentrated by ultrafiltration with PM10 membranes (Amicon, Danvers, MA) up to 50 mg/mL and then subjected to molecular sieve chromatography on Ultrogel AcA 44 (Reactifs IBF, Villeneuve-la-Garenne, France) equilibrated in H_2O buffer containing 0.15 M NaCl and 1 mM EDTA. A peak corresponding to a molecular weight of about 140 000 and representing about one-third of the total protein was discarded. The fractions of the second peak, M_r 70 000, were pooled and dialyzed against 5 × 10 volumes of buffer. The final concentration was in the range 7–15 mg/mL. Concentrations were determined with the Bio-Rad protein assay with bovine serum albumin as standard and were verified from the measurement of absorbance at 2800 Å, assuming an extinction coefficient of 14.7 (Mann & Elion, 1980). Our prothrombin preparations had a specific clotting activity ranging from 14 to 16 units/mg when assayed by the one-stage clotting assay (Caen et al., 1975). The error in protein concentration determination is about 5%.

Phospholipid Vesicle Preparation. Phosphatidylcholine (PC) and phosphatidylserine (PS) were from bovine spinal cord (grade 1, Lipid Products, Redhill, U.K.) and contained less than 1% impurities when analyzed by thin-layer chromatography. Vesicles containing 50% (w/w) PC and 50% (w/w) PS were prepared by extensive sonication followed by molecular sieve chromatography on Sepharose 4B according to Huang and Thompson (1974). Sonication was carried out at 0 °C on 40 mg/mL lipid in 5 mL of buffer for 2 h, under an argon stream, with a Branson Sonifier, Model 125, tuned for maximum power output and equipped with a standard probe. Fragments of the probe were eliminated by centrifugation at 100000*g* for 1 h at 4 °C. The dispersion was then subjected to upward-flow gel filtration. Vesicles were detected by recording turbidity at 2800 Å. In order to obtain monodisperse vesicles, only the four or five fractions corresponding to the top of the peak were kept and pooled. The vesicles were dialyzed against 5 × 10 volumes of buffer, and their concentrations were determined by assaying phosphorus (Bartlett, 1959) with a (w/w) conversion factor of 25, phospholipid/phosphorus (Nelsestuen & Lim, 1977). The error in phospholipid concentration determintion is probably not better than 15%. It is unlikely that the vesicles contain a significant proportion of lysolipids because the contrast match point of the vesicles alone would then be at a significantly higher D_2O content from that observed. Also, the variation of the contrast between lysolipids and solvent is sufficiently different so that the consistency found between our results at different contrasts assuming fully double chained lipids would be compromised by their presence. Finally, lysolipids have a destabilizing effect, yet our vesicles were stable for at least 1 week as judged by neutron scattering and gel filtration.

Complex Formation. The complex was formed by mixing different proportions of the lipid and protein solutions with $CaCl_2$ added to a final concentration of 3 mM. The buffer contained 0.2 M NaCl rather than the more physiological value of 0.15 M as this reduced protein aggregation in D_2O buffer.

Neutron Scattering

The neutron scattering profiles were measured on the small-angle scattering camera D11 (Ibel, 1976). The sample to detector distance was either 2.6 or 9.8 m, and the wavelength was 10 Å ($\Delta\lambda/\lambda$ = 8%; full width, half-maximum). The scattering curve and transmissions of each solution and corresponding solvent were measured. The scattering curve of the solute was obtained by subtracting the solvent scattering from the solution scattering, taking into account the small difference that is sometimes observed between the transmissions of solution and solvent. The scattering curve of water is obtained by subtracting the empty cell spectrum multiplied by the ratio of water transmission to the empty cell transmission from the measured water plus cell spectrum. The spectra were corrected for detector response and normalized by dividing by the water spectrum, which is isotropic under the conditions used. The water spectrum also provides the

calibration of the incident neutron flux.

Data Interpretation

In the small-angle limit, the scattering curve from monodisperse particles without correlations in position or orientation is approximated by the Guinier formula:

$$I(Q)/c = M_r(b/M_r - V\rho_s/M_r)^2 \exp(-R_G^2Q^2/3) \quad (1)$$

$Q = (4\pi \sin\theta)/\lambda$, with λ = the neutron wavelength and θ = half the scattering angle; $I(Q)$ = intensity of scattered neutrons divided by the sample thickness, the transmission, the incident neutron flux, and Avogadro's number; c = particle concentration; M_r = particle molecular weight; b/M_r = scattering length per unit molecular weight; V/M_r = solvent-excluded volume per unit molecular weight; ρ_s = solvent scattering density; R_G = whole particle radius of gyration. The contrast ρ between the particle and the solvent is given by $\rho = b/V - \rho_s$.

The above equation is valid in general for $QR_G \leq 1$ but extends further for more spherical objects; the extent of validity is determined experimentally. At a given contrast the plot of ln $I(Q)$ against Q^2 yields both R_G^2 and the value of $I(Q)$ at $Q = 0$, i.e., $I(0)$, by extrapolation. Usually b varies linearly with solvent D_2O content and thus so does $I(0)^{1/2}$. From a measurement of $I(0)$, M_r can be determined; the $I(0)$ in H_2O is usually used because there is then no error arising from the determination of the degree of D/H exchange. In these conditions an error of 5% in V results in half this error in the estimate of M_r of protein but about the same error with lipid.

Consider a monodisperse solution of lipid vesicles with a single bilayer to which protein attaches to form a lipid–protein complex. Measurements are made on the components separately prior to mixing and complex formation. The number n of protein molecules of molecular weight M_P bound to each lipid vesicle is the same. In the following the subscripts P, L, XL, XP, and X refer respectively to protein only, lipid vesicles only, complexed vesicles, complexed protein, and whole complex. With eq 1, the ratio of the scattering at $Q = 0$ from the complex to that from the vesicles alone is given by

$$\frac{I_X(0)}{I_L(0)} = \frac{c_{XL} + c_{XP}}{c_L} \frac{M_L}{M_{XL} + nM_P} \left(\frac{V_{XL}\rho_{XL} + nV_{XP}\rho_{XP}}{\rho_L V_L} \right)^2 \quad (2)$$

$I_L(0)$ is now normalized so that $c_{XL} = c_L$. Provided the partial specific volumes are unchanged by complex formation (i.e., $V_{XL} = V_L$; $V_{XP} = V_P$) and there is no coalescence of vesicles (i.e., $M_{XL} = M_L$), then as $c_{XP}/c_L = nM_P/M_L$ from the above equation the ratio of the molecular weights of the bound protein to lipid is given by

$$nM_P/M_L = (V_L\rho_L/M_L)(M_P/V_P\rho_P)(A - 1) \quad (3)$$

The ratio of the square root of the intensities has been replaced by A. When the complex is in the zero contrast condition, $A = 0$. On complex formation the partial specific volume of protein is unlikely to change significantly, but this is not necessarily true of the lipid.

When the protein is uniformly distributed over the vesicle surface and does not penetrate into the lipid, both layers can be considered to be separate, and the radii of gyration are related by $R_X^2 = f_{XL}R_{XL}^2 + f_{XP}R_{XP}^2$. f_{XL} and f_{XP} are the fractional scattering powers, $f_{XL} + f_{XP} = 1$, and $f_{XL} = (1 + nV_{XP}\rho_{XP}/V_{XL}\rho_{XL})^{-1}$; R_{XL} and R_{XP} are the radii of gyration of the vesicle and protein layer forming the complex. R_{XP} should remain constant once a sufficient number of protein molecules are bound to effectively form a uniform shell. If R_{XL} is equal to the radius of gyration of the vesicles alone (i.e., $R_{XL} = R_L$), then

$$R_{XP}^2 = (AR_X^2 - R_L^2)/(A - 1) \quad (4)$$

As all the quantities on the right-hand side of this equation can be measured, the radius of gyration of the protein shell alone can be determined, thus giving information about the protein distribution wihout recourse to model calculations as is necessary when the protein penetrates significantly into the lipid (Gogol & Engelman, 1984). Only if all three radii of gyration are known can eq 3 and 4 be combined to obtain the protein lipid ratio without knowledge of A.

The contrast is composed of two terms, one independent, I, and the other dependent, D, on the fraction F of the solvent composed of D_2O; i.e., $\rho = I + DF$. At infinite contrast, $1/\rho = 0$ and $F \rightarrow \infty$, the I terms are negligable so that $f_{XL} = (1 + nV_{XP}D_{XP}/V_{XL}D_{XL})^{-1}$. The radius of gyration of the complex when $1/\rho = 0$, $R_{G\infty}$, is only equal to the mechanical radius of gyration of a uniform particle with the same shape if $D_{XP} = D_{XL}$ and the dry volumes are close or proportional to the values calculated from the radial dimensions. When these restrictions are satisfied, $R_{GM}^2 = (V_{XL}R_{XL}^2 + nV_{XP}R_{XP}^2)/V_{XL} + nV_{XP})$, but in practice this equation is not valide as the first condition at least is not satisfied because $|D_{XL}| > |D_{XP}|$. The consequences of this depend on characteristics of the sample; for the complex studied in Figure 4 ($n \simeq 44$), $nV_{XP}D_{XP}/V_{XL}D_{XL} = 1.1$ approximately giving $R_{G\infty}^2 = 0.47R_{XL}^2 + 0.53R_{XP}^2$ whereas $R_{GM}^2 = 0.1R_{XL}^2 + 0.9R_{XP}^2$. The prefactors have been obtained from information supplied under Results and with the equation for the radius of gyration of a uniform spherical sheel, $R_G^2 = 0.6(r_2^5 - r_1^5)/(r_2^3 - r_1^3)$, where r_2 and r_1 are respectively the outer and inner radii. Hence when the protein is bound to the lipid exterior, $R_{XL} < R_{XP}$, and the measured value of $R_{G\infty}$ is significantly smaller than R_{GM} and therefore cannot be used to deduce the inner and outer radii of the complex. This problem has been discussed at length by Witz (1983) and considered by others (Zaccai & Jacrot, 1983).

The protein binding data were analyzed by fitting them to the following equation assuming a single class of equivalent noninteracting binding sites:

$$1/n = (1/F)(K_D/n_{max}) + 1/n_{max} \quad (5)$$

where n_{max} is the maximum number of protein molecules bound per vesicle, K_D is the dissociation constant, and F is the concentration of free protein. $F = C_T - nC_V$, the concentration of total protein minus that bound to lipid; C_V is the concentration of the vesicles.

In Figures 1 and 2 the statistical error is smaller or equal to the size of the points plotted. This is also true in Figure 3 as only the relative error is important for this plot. The values given in the text include an estimate of errors from all sources.

Results and Discussion

Prothrombin Solutions. Figure 1 shows typical plots of ln $I(Q)$ against Q^2 obtained from solutions of human prothrombin. From the straight line fits the radii of gyration, R_G, and $I(0)$ are obtained. In H_2O buffer the plot is linear to the lowest angles measured in accordance with the Guinier approximation, but in D_2O buffer there is a weak upswing in intensity at low Q. The latter observation testifies to the presence of a small proportion of aggregates which could be reduced but not completely removed by centrifugation at different ionic strengths and Ca^{2+} concentrations. The radii of gyration were the same within experimental accuracy

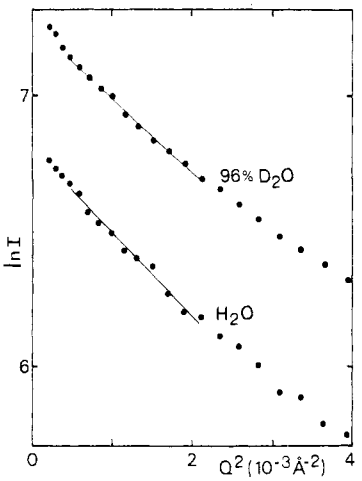

FIGURE 1: Guinier plots of the low-angle scattering obtained from solutions of prothrombin in H_2O and 96% D_2O buffer. The concentrations were respectively 7.5 and 4.4 mg·mL^{-1}, and the R_G = 30.5 ± 1 and 28.6 ± 1 Å.

without calcium or with up to 4 mM Ca^{2+} added.

The plot of $I(0)^{1/2}$ against the buffer D_2O content intercepts the ordinate at 42.7 ± 0.5% D_2O, which is therefore the zero contrast condition (ρ_P = 0). This is close to the value calculated from the amino acid and polysaccharide (~10%) compositions and scattering length densities (Jacrot & Zaccai, 1981; Perkins et al., 1981). Assuming that between 80% and 100% of the labile hydrogens exchange with solvent deuterium, the dry and partial specific volumes are respectively 89 000 ± 3000 Å^3 and 0.745 ± 0.025 mL·g^{-1}. Using the intensity in H_2O buffer, because the errors are minimized, the molecular weight is estimated to be 72 000 ± 5000, which is in agreement with sequencing and other studies (Mann et al., 1981).

The plot of the radius of gyration squared, R_G^2, against inverse contrast, $1/\rho$ (Stuhrmann plot), can be fitted to a straight line with a positive slope [$\alpha = (2.4 \pm 0.25) \times 10^{-4}$] as is generally obtained from globular proteins because the higher scattering density hydrophilic amino acids are predominantly near the surface (Ibel & Sturhmann, 1975). The interecept at infinite contrast ($1/\rho$ = 0) is 29.5 ± 1 Å. A sphere with the measured dry volume would have a radius of gyration of only 21.5 Å so the prothrombin molecule must be elongated. A prolate ellipsoid similar in dimensions to that proposed by Lamy and Waugh (1953) with a semiaxis of approximately 60 × 20 × 20 Å has a radius of gyration and volume similar to those measured here. This is but one of many possible structures compatible with the neutron scattering data and indeed is very unlikely to give an accurate representation in view of the domain struture of the molecule. The structure proposed by Lim et al. (1977) consisting of a linear arrangement of three spheres corresponding to fragment 1, fragment 2, and prethrombin 2, however, has a R_G (i.e., ~36 Å) that is too large. If the sphere representing fragment 1 is replaced by the disc shape found with crystallography (Park & Tulinsky, 1986) and having its short axis aligned through the centers of the remaining two spheres, the calculated R_G is reduced to ~33 Å. Compacting the structure by allowing for some merger between fragments would be sufficient to give the measured R_G and a total length compatible with that measured below for the protein shell. The radius of gyration and molecular weight reported here are smaller by at least 3 Å and 2000, respectively, than were measured with X-ray scattering (Osterberg et al., 1980). Also, we found no evidence for the large calcium-induced conformational change signalized by the latter technique.

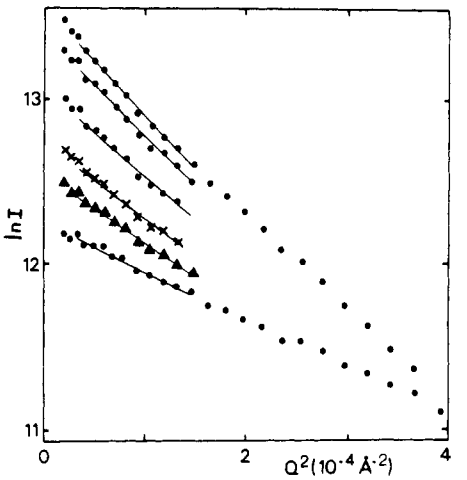

FIGURE 2: Guinier plots of the low-angle scattering obtained from vesicles and vesicle–prothrombin complexes in 95% D_2O buffer. The lower curve was obtained from the vesicles alone, and the succeeding curves were obtained with added protein concentrations of successively 0.5, 1.0, 2.0, 3.0, and 5.0 mg·mL^{-1}. The concentration of lipid was 1.5 mg·mL^{-1} in all cases. The slopes give the radii of gyration, R_G, and the values of $I(0)$ are obtained by extrapolation. Measuring times were of the order of 15 min each. A disadvantage of the technique is that most measurements on the complex were made at prothrombin concentrations that are much higher than physiological, i.e., ~0.1 mg·mL^{-1}. The concentrations in D_2O buffer could be reduced by a factor of up to about 10, but at other contrasts a decrease of this order would result in unacceptably long measuring times.

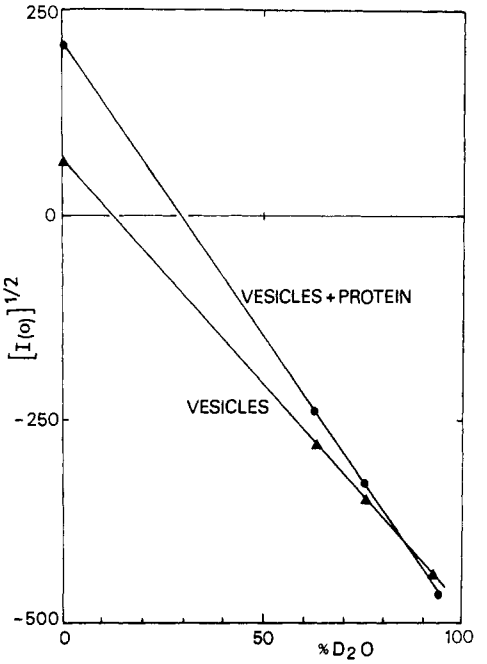

FIGURE 3: Variation as a function of buffer D_2O content of the square root of $I(0)$ divided by the total concentration, sample thickness, and transmission for vesicles alone and complex. The concentration of the vesicles alone varied between 0.5 and 14.0 mg·mL^{-1}; no concentration-dependent effects were observed. The complex was formed from a solution containing 1.5 mg·mL^{-1} lipid and 3.0 mg·mL^{-1} prothrombin.

Vesicles. The lowest intensity plot in Figure 2 is an example of the neutron scattering near the Guinier range obtained from phosphatidylcholine–phosphatidyleserine (1:1 w/w) single bilayer vesicles. Figure 3 shows that the plot of $I(0)^{1/2}$ against the buffer D_2O content is linear with the zero contrast condition occurring at 13.0 ± 0.5% D_2O from which the average dry volume peer lipid and partial specific volume are calculated respectively to be 1400 ± 140 Å^3 and 1.05 ± 0.10 mL·g^{-1}. This dry volume is similar to that found for micelles of dihexa-

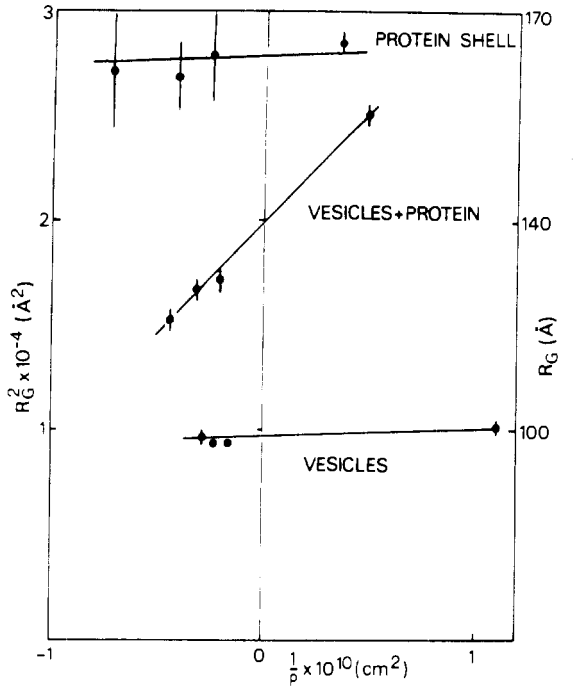

FIGURE 4: Square of the measured radius of gyration of vesicles ($R_G = R_L$) and complex ($R_G = R_X$) versus the reciprocal of the contrast, $1/\rho$. The radius of gyration squared for the protein shell ($R_G = R_{XP}$) is also plotted and was obtained from eq 4. Again, no concentration-dependent effects were observed.

noylphosphatidylcholine (Chen, 1986) after taking the difference in chain length into account. The molecular weight of a liposome, using the value of $I(0)$ measured in H_2O buffer, is estimated to be $(1.6 \pm 0.32) \times 10^6$, which corresponds to 2100 ± 420 lipid molecules per vesicle. The large error in the estimate for the molecular weight is mostly due to the uncertaity in the absolute lipid concentration.

The molecular weight and dimensions (see below) of the vesicles are about the smallest physically possible. This suggests that they are rather monodisperse as larger vesicles would contribute disproportionately to scattering (eq 1) and therefore, even if their concentration be relatively minor, give rise to a significant increase in the measured values of $I(0)$ and R_G. Furthermore, scattering curves measured to higher angles show a first and a weak second subsidiary maximum (measurements were not extended beyond this range), again indicating that the system is monodisperse to a good approximation.

Figure 4 shows that the plot of R_L^2 against inverse contrast is nearly flat [$\alpha = (9.1 \pm 5.0) \times 10^{-4}$], which indicates that there is little asymmetry in scattering density across the lipid bilayer (Gogol & Engelman, 1984). The intercept at infinite contrast ($1/\rho = 0$) is 97 ± 2 Å (Figure 4). The width of the bilayer cannot be deduced directly from the data presented here; however, the thickness in lecithin vesicles with liquid-like chains (Reiss-Husson, 1967; Luzzti, 1968; Torbet & Wilkins, 1976) including sonicated vesicles (Wilkins et al., 1970) has been measured to be about 40 Å. A spherical shell with the latter width and outer radius of 114 ± 3 Å would have the same radius of gyration as that measured. The interdependence of the vesicle radius of gyration and bilayer width is such that the estimated area per molecule depends little on the bilayer thickness used. The average area per molecule found, 110 ± 18 Å^2, is similar to that in very small micelles of lecithin with short hydrocarbon chains (Chen, 1986) but significantly larger than past estimates for highly hydrated lipid bilayers with liquid crystalline chains. For example, the upper limits to the area of egg lecithin in a lamellar phase and dimyristoyllecithin vesicles have been estimated to be 72 Å^2 (Reiss-Husson, 1967; Luzzati, 1968) and 78 Å^2 (Watts et al., 1978), respectively. A mixture of charged and uncharged phospholipids of unknown composition extracted from human brain was found to have a maximum area of 80 Å^2 per lipid (Luzzati & Husson, 1962). The relatively large area found for the small vesicles under study here could be a consequence of their high curvature. The large charge density due to the 50% phosphatidylserine does not seem to be a contributory factor as the addition of calcium up to 4 mM did not alter the radius of gyration. The extrapolated intensity at $Q = 0$, $I(0)$, did not change with time and was also unaffected by calcium, which shows that vesicle fusion was negligible over the period of measurement.

Prothrombin/Lipid Complex. The low-angle scattering as a function of contrast was measured from solutions containing a ratio of lipid to prothrombin of 1/2 (w/w). It is shown later that at this ratio in the presence of calcium the vesicles are loaded to 75% of the maximum possible. The resulting values of $I(0)^{1/2}$ normalized to total concentration (lipid + protein) are plotted in Figure 3. The value of $I(0)^{1/2}$ at the zero contrast condition for the protein ($\rho_P = 0$ in 43% D_2O) normalized to the lipid concentration is equal within experimental error to that obtained from the vesicles alone at the same contrast (Figure 3). Similarly, the radius of gyration at $\rho_P = 0$ (Figure 4; $1/\rho_X = -1.05 \times 10^6$ Å^2 when $\rho_P = 0$) is very close to that of the lipid alone. These results demonstrate that the protein has little effect on vesicle dimensions, and consequently, its penetration into the lipid phase must be very limited (Lim et al., 1977; Dombrose et al., 1979; Mayer et al., 1983).

On addition of an excess of EDTA to the D_2O sample, $I(0)$ and R_G reverted, within experimental error, to the values given by the lipid alone. (The values of these parameters from the free protein are much smaller than those from the lipid, and therefore, they contribute little to the scattering in the Q range of interest.) This shows that protein binding is both reversible and negligible in the absence of free calcium. Additionally, the coalescence of vesicles or the sequestration of protein within them can only occur to a small extent if at all (Lim et al., 1977; Dombrose et al., 1979).

The zero contrast condition for this complex occurs at 29.0 ± 0.5% D_2O (Figure 3) from which the ratio of bound protein to lipid, nM_P/M_L, is estimated to be 1.9 ± 0.1. Thus as a value of 2 indicates that all protein is bound, then all or nearly all of the prothrombin is attached to the vesicles.

The Stuhrmann plot in Figure 4 of the data obtained at a 1:2 lipid to protein ratio gives a radius of gyration at infinite contrast $R_{LP\infty}$ ($1/\rho_{LP} = 0$) of 140 Å and a positive slope [$\alpha = (1.05 \pm 0.2) \times 10^{-2}$] because the component with the highest scattering density (Ibel & Stuhrmann, 1975), the protein, is attached on the outside of the vesicle. The large difference in the variation of H/D exchange between lipid and protein results in $R_{LP\infty}$ being smaller than that of a particle with the same shape and volume but which undergoes homogeneous exchange. Therefore, the estimate of $R_{LP\infty}$ cannot be used as though it were equivalent to the mechanical radius of gyration.

Because the radius of gyration of vesicles is very similar when they are alone or complexed, the use of eq 4 to estimate the radius of gyration of the external protein layer is justified. The results show (Figure 4) that R_{XP} is almost invariant with contrast ($\alpha \simeq 0$, $R_{XP\infty} = 168 \pm 3$ Å at all contrasts), which indicates that there is little radial change in scattering density across the protein shell (Ibel & Stuhrmann, 1975). The γ-carboxyglutamate residues and two of the carbohydrate chains

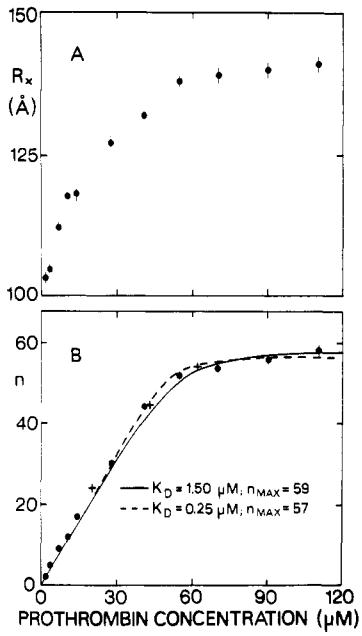

FIGURE 5: (A) Variation of the complex radius of gyration, R_X, in D_2O buffer as a function of prothrombin concentration when the lipid concentration was 1.5 mg·mL^{-1}. (B) Number of prothrombin molecules, n, bound per lipid vesicle as a function of prothrombin concentration: (●) obtained in 95% D_2O buffer; (+) obtained in H_2O buffer. Measurements made in 63% and 76% D_2O buffers at a protein/lipid (w/w) ratio of 2/1 coincide with those plotted and are not shown. The concentration of lipid was 1.5 mg·mL^{-1}; a few points were also measured up to 4.5 mg·mL^{-1} lipid with a proportionate increase in protein concentration which gave the same results on normalization. The fits were calculated with eq 5, using the dissociation constants, K_D, and the number of prothrombin molecules bound at saturation, n_{max}, shown.

(the third is attached to prothrombin 2, which is nearer to the middle of the elongated protein) have a higher than average scattering density and form part of fragment 1. This is the region that binds to lipid and is therefore positioned nearer to the center of the complex than the rest of the protein. Hence a small negative slope to the Stuhrmann plot is possible in theory. However, it is doubtful that the data and the reliability of eq 4 could be good enough to show this.

The outer radius of the lipid shell was estimated above to be about 114 Å, and as the protein shell behaves as a uniform scatterer (Figure 4), the equation for the radius of gyration of a uniform hollow sphere can be used to obtain the outer radius of the protein layer, i.e., ~200 Å. This puts the thickness of the protein shell at about 90 Å as reported by Lim et al. (1977). The radius of gyration of prothrombin in solution indicates that the molecule is elongated with a maximum length of about 120 Å in the unlikely event of it being a simple prolate ellipsoid. As discussed above the structure is probably more compact. In any event the long axis of the prothrombin molecule must be relatively perpendicular to the lipid surface in order to make a shell as wide as 90 Å.

The variation of the complex radius of gyration, R_X, and intensity at $Q = 0$, $I_X(0)$, were measured over a wide range of protein/lipid ratios in 95% D_2O buffer (Figure 2) and at three ratios in H_2O buffer. The measured values of R_X in 95% D_2O are plotted in Figure 5A, and the number, n, of prothrombin molecules bound per vesicle shown in Figure 5B was obtained from $I_X(0)$ with eq 3 and the ratio of the molecular weights of a prothrombin molecule to that of a vesicle, M_P/M_L. Up to about 44 prothrombin molecules per vesicle ($nM_P/M_L \simeq 2$), the binding curve is nearly straight and almost all of the protein is bound (Figure 5B); thereafter, the curve bends round giving a saturation value for n of 57 ± 7. The area on the lipid surface per protein molecule is therefore 2900 ± 400 Å^2, and as 68% of the lipid is on the outside of the bilayer, the number of lipid molecules potentially interacting with a protein molecule is 25 ± 6. The values of n do not depend on the buffer D_2O content, which demonstrates that the small proportion of aggregates found with prothrombin in D_2O buffer (Figure 1) did not distort the protein binding measurements.

The area per protein molecule at saturation is more than twice that projected on to the surface by a prolate ellipsoid of dimensions 20 × 20 × 60 Å oriented with its long axis extended radially. However, the structure of fragment 1 is known to high resolution (Park & Tulinsky, 1986) with the exception of the disordered carbohydrate chains and amino-terminal region where the 10 γ-carboxyglutamic acid residues are located. The overall shape is disc-like with a diameter and thickness of 60 Å and 22 Å, respectively. Thus if fragment 1 is oriented so to cover the lipid approximately to the maximum extent, allowing for packing defects, the required area would be near to the value obtained at saturation binding. This circumstantial evidence suggests that prothrombin binding is limited largely by physical obstruction. Lim et al. (1977) came to a similar conclusion, but the amount of protein bound and the area available to each molecule are much smaller. Structures with the fragment 1 disc facing the lipid and the remaining about 70% of the molecule extending outward from it can be constructed that would have the required radius of gyration and an overall length equal to that of the measured thickness of the protein shell.

Both the measured value of the complex radius of gyration (Figure 5A) and the number of prothrombin molecules bound per vesicle (Figure 5B) attain saturation at about the same protein concentration. The calculated R_{XP} values from the data in Figure 5A and eq 4 are constant within experimental error with the possible exception of the two lowest concentrations where the error is largest. Thus, the behavior of the calculated R_{XP} is consistent with a centrosymmetric complex that does not change dimensions as a function of the amount of protein bound. In Figure 5B the binding curves calculated from eq 5 with two extreme values for the apparent dissociation constant (0.2 and 1.5 μM) are compared with the measured curve. At low protein concentrations both dissociation constants give curves that are the same at the resolution of relevance here; above about 30 μM protein the shape of the curve with the higher K_D value is too rounded while the other is too sharp to fit the data optimally (Figure 5B). The best fits are obtained with an apparent dissociation constant within the range $K_D = 0.8 \pm 0.4$ μM.

The binding of prothrombin and its fragment 1 to various lipid mixtures in the form of monolayers, stacked multilayers, and single-bilayer vesicles has been investigated by a number of different techniques as shown by the following examples. The high-affinity binding sites are not considered as they have only been observed in conditions (Kop et al., 1984) that are not under investigation here. Monolayers have been made on the air–buffer interface (Mayer et al., 1983; Lecompte et al., 1980) and on chromium-coated substrates (Kop et al., 1984). The former were studied with radioactivity labeled protein or by monitoring the surface pressure changes while with the latter ellipsometry (an optical reflection technique) was used. Kop et al. (1984) have considered these results in detail. Monolayers suffer from the drawback that there are always doubts, greater than those for bilayers, about how closely they represent the behavior of lipids in biomembranes. Also surface pressure and substrate interactions may have an effect that

could be be difficult to assess. Although in a comparative experiment the thrombin-generating capacity of monolayers on a chromium substrate and single-bilayer vesicles was judged to be comparable (Kop et al., 1984), this does not necessarily indicate that the binding of prothrombin alone is alike in both systems as these experiments were performed in the presence of factors V_a and X_a. Multilayers that have been studied with ellipsometry (Cuypers et al., 1983) suffer from the inherent disadvantage that the proximity of adjacent bilayers could lead to modification of protein binding due to intermembrane interactions. For example, interdigitation of the extended prothrombin molecules on different bilayers could impede binding.

The binding of prothrombin to single-bilayer vesicles provides the best pure lipid approximation to biomembranes. However, most techniques work best with vesicles that are small and monodisperse or at least have a known degree of polydispersity. Such samples cannot be readily made or characterized; also, their high curvature might modify the protein–lipid interaction, but there is evidence to discount this possibility (Nelsestuen & Lim, 1977). Light scattering measurements have yielded a saturation load of 1.2 g of prothrombin/g of lipid, a binding constant K_D of 1 μM (Nelsestuen & Broderius, 1977), and a change in thickness due to prothrombin binding of 85 Å (Lim et al., 1977). The maximum binding is less than half the value we find, but there is rather good agreement in the latter two numbers. The projected area per protein, 1830 Å^2 (Lim et al., 1977), is much smaller than ours. This difference is probably at least partly due to an overestimate in the vesicle molecular weight because with the dimensions quoted (Lim et al., 1977) the area per lipid is smaller than is physically reasonable. Recalculation using the vesicle dimensions and density given (Lim et al., 1977) yields an area per protein of 3000 Å^2 as found above, but the agreement is deceptive because there are far fewer proteins bound. Gel filtration has been used in conjunction with measurements of turbity and radioactivity (Dombrose et al., 1979) to monitor the binding of fragment 1 to vesicles similar in size to those we used but containing phosphatidylglycerol as the negative charged lipid. The binding constant, the number of bound protein molecules at saturation, and the projected area per protein are all close to the values we obtain at similar calcium concentrations. These results do, however, suffer from the weakness that neither the molecular weight nor the size of the vesicles was directly measured. One advantage of the neutron scattering measurements is that both the molecular weight and the dimensions of vesicles and complexes are measured. In conclusion, our estimates using vesicles for the apparent dissociation constant (Nelsestuen & Broderius, 1977; Dombrose et al., 1979) and thickness of the protein layer (Lim et al., 1977) are in good agreement with previous estimates, while there is some discord on the area/protein on the lipid surface at saturation; we and Dombrose et al. (1979) find a similar value that is about double that reported by Lim et al. (1977).

ACKNOWLEDGMENTS

We thank Institut Laue-Langevin staff, particularly those people involved in running D11.

REFERENCES

Bartlett, G. R. (1959) *J. Biol. Chem. 234*, 466–468.
Borowski, M., Furie, B. C., Goldsmith, G. H., & Furie, B. (1985) *J. Biol. Chem. 260*, 9258–9264.
Caen, J., Larrieu, M. J., & Samama, M. (1975) *L'Hemostase*, Expansion Scientifique, Paris.
Chen, S. H. (1986) *Annu. Rev. Phys. Chem. 37*, 351–399.
Cupers, P. A., Corsel, J. W., Janssen, M. P., Kop, J. M. M., Hermens, W. T., & Hemker, H. C. (1983) *J. Biol. Chem. 258*, 2426–2431.
Dombrose, F. A., Gitel, S. N., Zawalich, K., & Jackson, C. M. (1979) *J. Biol. Chem. 254*, 5027–5040.
Freyssinet, J.-M., Thevenon, D., Souque, A., & Suscillon, M. (1982) *Thromb. Haemostasis 48*, 120–124.
Gogol, E. P., & Engelman, D. M. (1984) *Biophys. J. 46*, 491–495.
Heldebrant, C. M., Butkowski, R. J., Bajaj, S. P., & Mann, K. G. (1973) *J. Biol. Chem. 248*, 7149–7163.
Huang, C., & Thompson, T. E. (1974) *Methods Enzymol. 32*, 485–489.
Ibel, K. (1976) *J. Appl. Crystallogr. 9*, 296–309.
Ibel, K., & Stuhrmann, H. B. (1975) *J. Mol. Biol. 93*, 255–265.
Jackson, C. M., & Nemerson, Y. (1980) *Annu. Rev. Biochem. 49*, 765–811.
Jacrot, B., & Zaccai, G. (1981) *Biopolymers 20*, 2413–2426.
Kop, J. M. M., Cuypers, P. A., Lindhout, T., Hemker, H. C., & Hermens, W. T. (1984) *J. Biol. Chem. 259*, 13993–13998.
Kruse, J., Timmins, P. A., & Witz, J. (1982) *Virology 119*, 42–50.
Laemmli, U. K. (1970) *Nature (London) 277*, 680–685.
Lamy, F., & Waugh, D. F. (1953) *J. Biol. Chem. 203*, 489–499.
Lecompte, M.-F., Miller, I. R., Elion, J., & Benarous, R. (1980) *Biochemistry 19*, 3434–3439.
Lentz, B. R., Alford, D. R., Jones, M. E., & Dombrose, F. A. (1985) *Biochemistry 24*, 6997–7005.
Lim, T. K., Bloomfield, V. A., & Nelsestuen, G. L. (1977) *Biochemistry 16*, 4177–4181.
Luzzati, V. (1968) In *Biological Membranes* (Chapman, D., Ed.) pp 71–123, Academic, New York.
Luzzati, V., & Husson, F. (1962) *J. Cell Biol. 12*, 207–219.
Mann, K. G. (1984) *Prog. Hemostasis Thromb. 7*, 1–23.
Mann, K. G., & Elion, J. (1980) in *CRC Handbook Series in Clinical Laboratory Science* (Seligson, D., Ed. in Chief) Section 1, Vol. III (Schmidt, R. M., Ed.) pp 15–31, CRC Press, Boca Raton, FL.
Mann, K. G., Elion, J., Butkowski, R. J., Dowing, M., & Nesheim, M. E. (1981) *Methods Enzymol. 80*, 286–302.
Mayer, L. D., & Nelsestuen, G. L. (1981) *Biochemistry 20*, 2457–2463.
Mayer, L. D., Nelsestuen, G. L., & Brockman, H. L. (1983) *Biochemistry 22*, 316–321.
Nelsestuen, G. L. (1976) *J. Biol. Chem. 251*, 5648–5656.
Nelsestuen, G. L., & Broderius, M. (1977) *Biochemistry 16*, 4172–4177.
Nelsestuen, G. L., & Lim, T. K. (1977) *Biochemistry 16*, 4164–4171.
Nesheim, M. E., & Mann, K. G. (1983) *J. Biol. Chem. 258*, 5386–5391.
Osterberg, R., Sjoberg, B., Osterberg, P., & Stenflo, J. (1980) *Biochemistry 19*, 2283–2286.
Owen, W. G., Esmon, C. T., & Jackson, C. M. (1974) *J. Biol. Chem. 249*, 594–605.
Park, C. H., & Tulinsky, A. (1986) *Biochemistry 25*, 3977–3982.
Perkins, S., Miller, A., Hardingham, T. E., & Muir, H. (1981) *J. Mol. Biol. 150*, 69–95.
Prigent-Dachary, J., Faucon, J.-F., Boisseau, M.-R., & Dufourcq, J. (1986) *Eur. J. Biochem. 155*, 133–140.
Reiss-Husson, F. (1967) *J. Mol. Biol. 25*, 363–382.

Resnick, R. M., & Nelsestuen, G. L. (1980) *Biochemistry 19*, 3028–3033.
Torbet, J., & Wilkins, M. H. F. (1976) *J. Theor. Biol. 62*, 447–458.
Van der Waart, P., Hemker, H. C., & Lindhout, T. (1984) *Biochemistry 23*, 2838–2842.
Watts, A., Marsh, D., & Knowles, P. F. (1978) *Biochemistry 17*, 1792–1801.
Wilkins, M. H. F., Blaurock, A. E., & Engleman, D. M. (1971) *Nature (London) New Biol. 230*, 72–76.
Witz, J. (1983) *Acta Crystallogr., Sect. A: Found. Crystallogr. A39*, 706–711.
Zaccai, G., & Jacrot, B. (1983) *Annu. Rev. Biophys. Bioeng. 12*, 139–157.

Rapid Degradation of D- and L-Succinimide-Containing Peptides by a Post-Proline Endopeptidase from Human Erythrocytes†

Jamil Momand and Steven Clarke*
Department of Chemistry and Biochemistry and The Molecular Biology Institute, University of California, Los Angeles, California 90024

Received May 8, 1987; Revised Manuscript Received July 13, 1987

ABSTRACT: We have been interested in the metabolic fate of proteins containing aspartyl succinimide (Asu) residues. These residues can be derived from the spontaneous rearrangement of Asp and Asn residues and from the spontaneous demethylation of enzymatically methylated L-isoAsp and D-Asp residues. Incubation of the synthetic hexapeptide *N*-Ac-Val-Tyr-Pro-Asu-Gly-Ala with the cytosolic fraction of human erythrocytes resulted in rapid cleavage of the prolyl–aspartyl succinimide bond producing the tripeptide *N*-Ac-Val-Tyr-Pro. The rate of this reaction is equal for both L- and D-Asu-containing peptides and is 10-fold greater than the rate of cleavage of a corresponding peptide containing a normal Pro–Asp linkage. When the aspartyl succinimide ring was replaced with an isoaspartyl residue, the cleavage rate was about 5 times that of the normal Pro-Asp peptide. The tripeptide-producing activity copurified on DEAE-cellulose chromatography with an activity that cleaves *N*-carbobenzoxy-Gly-Pro-4-methylcoumarin-7-amide, a post-proline endopeptidase substrate. These two activities were both inhibited by an antiserum to rat brain post-proline endopeptidase, and it appears that they are catalyzed by the same enzyme. This enzyme has a molecular weight of approximately 80 000 and is covalently labeled and inhibited by [^{3}H]diisopropyl fluorophosphate. The facile cleavage of the succinimide- and isoaspartyl-containing peptides by this post-proline endopeptidase suggests that it may play a role in the metabolism of peptides containing altered aspartyl residues.

The thermodynamic instability of proteins at physiological pH and temperature results in the spontaneous formation of a number of covalently altered derivatives of amino acid residues. Two of the least stable residues are aspartic acid and asparagine because they can be involved in deamidation, isomerization, and racemization reactions that result in the formation of D- and L-succinimidyl, D- and L-isoaspartyl, and D- and L-aspartyl residues (Ahern & Klibanov, 1985; Brunauer & Clarke, 1986; Di Donato et al., 1986; Geiger & Clarke, 1987). There is evidence that proteins and peptides containing at least two of these derivatives, L-isoaspartyl and D-aspartyl residues, can be methyl esterified by widely distributed protein methyltransferases (Clarke, 1985). In synthetic peptides these esters have been shown to be nonenzymatically demethylated to succinimide residues, which can then be hydrolyzed to give a mixture of D- and L-isoaspartyl and D- and L-aspartyl residues (Murray & Clarke, 1986; McFadden & Clarke, 1987). Although the cellular role of the protein methyltransferase is not understood, it has been proposed that this enzyme may function in the repair of altered proteins because it can catalyze the conversion of isoaspartyl residues in peptides to aspartyl peptides in moderate yield (Johnson et al., 1987; McFadden & Clarke, 1987).

In this study we have focused on an alternative pathway for the metabolism of proteins containing atypical aspartate derivatives. We were interested in examining the possibility that specific enzymes may catalyze the proteolysis of these species. We have used the synthetic peptide *N*-Ac-Val-Try-Pro-Asp-Gly-Ala as a prototype on which to build a series of abnormal peptides where the aspartyl residue is replaced with a D-succinimide, L-succinimide, D-isoaspartyl, or L-isoaspartyl derivative. Each peptide was then used as a model to explore the proteolytic metabolism of these altered protein structures in cell extracts. We have found that when these peptides are incubated with human erythrocyte cytosol, the Pro–X bond is rapidly cleaved by an activity that is immunologically related to a post-proline endopeptidase isolated from rat brain (Andrews et al., 1982). Post-proline endopeptidase has been described as a serine protease in several nonerythroid mammalian tissues that exists as a single polypeptide of approximately 70 000 daltons and an optimal activity observed between pH 7.5 and pH 8.0 (Rupnow et al., 1979; Walter et al., 1980). Interestingly, in our studies, the human erythrocyte enzyme was found to cleave the abnormal hexapeptides at a faster rate than the hexapeptide containing the normal Pro–Asp bond. The fact that the altered peptide is recognized as a better substrate than the normal substrate indicates that proteases may prefer damaged proteins over normal proteins and se-

† This work was supported by National Institutes of Health Grants GM-26020 and EY-04912 and by a Grant-in-Aid from the American Heart Association with funds contributed in part by the Greater Los Angeles Affiliate.
* Correspondence should be addressed to this author.

0006-2960/87/0426-7798$01.50/0